



Overview of ALICE results

Antonio Ortiz Velasquez
on behalf of the ALICE Collaboration

*Instituto de Ciencias Nucleares, Universidad Nacional Autónoma de México.
Circuito exterior s/n, Ciudad Universitaria, Del. Coyoacán, C.P. 04510, México DF.*

Abstract

The ALICE detector was designed to study the physics of matter under extreme conditions of high energy density. Different results were reported by the experiment using data from the successful run I of the LHC. The goal of the present work is to present an overview of recent ALICE results. This comprises selected results from several analyses of pp, p-Pb and Pb–Pb data at the LHC energies.

Keywords:

sQGP, heavy ion collisions, proton nucleus reaction, LHC, collectivity.

1. Introduction

Matter which surrounds us can be found in a variety of phases, the changes on its external conditions allows to go from one to another phase. From lattice QCD, it is predicted that hadronic matter under extreme conditions of high temperature and density changes its properties, in this state the fundamental degrees of freedom are given by quarks and gluons [1]. The phase transition occurs at a critical (crossover) temperature between 143–171 MeV [2, 3, 4, 5, 6, 7]. The experimental access to explore and test the QCD phase diagram and to address the fundamental question of hadron confinement and chiral symmetry breaking is via ultra-relativistic heavy ion collisions.

The hot and dense matter has been studied in the Relativistic Heavy Ion Collider (RHIC) at Brookhaven National Lab, the collisions of Au–Au at $\sqrt{s_{NN}} = 0.2$ TeV produced a perfect fluid that is initially closer to the ideal hydrodynamic limit, a theoretical scenario in which the viscosity is zero. This result has been confirmed by experiments at the Large Hadron Collider, where Pb–Pb collisions at $\sqrt{s_{NN}} = 2.76$ TeV have been achieved [8]. ALICE (A Large Ion Collider Experiment) is the only experiment at the LHC designed for

this purpose[9]. It has collected data which correspond to an integrated luminosity of $\approx 10\mu\text{b}^{-1}$ and $\approx 0.1\text{nb}^{-1}$ during the successful runs of 2010 and 2011, respectively. For the hot nuclear matter effects to be studied, analyses of pp and p-Pb data were also performed. Unexpectedly, these data revealed intriguing effects which are not well understood. In this paper, a review of selected results of ALICE will be presented, this comprises several measurements in different colliding systems, pp, p-Pb and Pb–Pb.

2. The ALICE apparatus

Particle identification (PID) is an important tool to study the hot and dense matter created in relativistic heavy ion collisions. That is why ALICE is an experiment specialized in PID from hundreds of MeV/c up to tens of GeV/c. The central barrel of ALICE is placed inside a large solenoidal magnet which provides a magnetic field of 0.5 T. It is dedicated to detect hadrons, electrons, and photons produced at mid-pseudorapidity, $|\eta| < 0.8$. It comprises an Inner Tracking System (ITS) of high-resolution silicon detectors, a cylindrical Time-Projection Chamber (TPC), and particle identification arrays of Transition-Radiation Detectors (TRD) and of

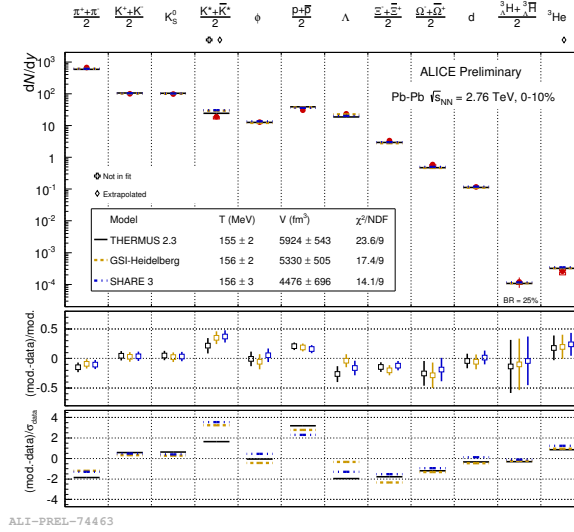


Figure 1: Thermal fits of particle yields in 0-10% Pb–Pb collisions.

Time-Of-Flight (TOF) counters. Additional central sub-systems, not-covering full azimuth, are a ring-imaging Cherenkov detector for High-Momentum Particle Identification (HMPID), and two electromagnetic calorimeters: a high-resolution PHOTon Spectrometer (PHOS) and a larger-acceptance ElectroMagnetic Calorimeter (EMCal). The muon arm detects muons emitted within $2.5 < \eta < 4$ and consists of a complex arrangement of absorbers, a dipole magnet, five pairs of tracking chambers, and two trigger stations. Several smaller detectors (VZERO, TZERO, FMD, ZDC, and PMD) for triggering, multiplicity measurements and centrality determination are installed in the forward region.

3. Latest progress on the study of the hot and dense matter

In central heavy ion collisions at ultra relativistic energies it is well established that a strongly interacting medium of quarks and gluons is created. To learn about the early state of the system, low p_T (< 2.2 GeV/c) direct photons are used. A temperature of 304 MeV has been measured for the 0-40% Pb–Pb collisions [10]. Hence, the system at the LHC is hotter than that produced at RHIC, where an early temperature of 221 MeV was measured for the 0-20% Au-Au collisions. The system created at the LHC is also denser, the average multiplicity per number of participant is two times that measured at RHIC [11]. Also interesting is the fact that the same centrality dependence is found at RHIC and LHC.

The system expands and cools down, when the inelastic interactions cease the yields of particles are fixed. This is the stage of the so-called chemical freeze-out which is studied using the yields of identified hadrons. As illustrated in Fig. 1, within 20% hadrons (except K^*) are described by thermal models with a common chemical freeze-out temperature $T_{\text{ch}} \approx 156$ MeV. However, larger deviations are observed for protons and K^* , for the latter, this is not a surprise since its mean lifetime is comparable to that for the fireball (≈ 10 fm/c) [13]. As discussed here [14], the statistical model is an effective model and the small deviations from the equilibrium picture may simply indicate that the precision of the data has become sufficient to reveal its limitations.

The transverse momentum distributions of identified hadrons contain valuable information about the collective expansion of the system ($p_T \lesssim 2$ GeV/c), the presence of new hadronization mechanisms like quark recombination ($2 \lesssim p_T \lesssim 8$ GeV/c) [15] and, at larger transverse momenta, the possible modification of the fragmentation due to the medium [16, 17]. ALICE has reported the transverse momentum spectra, as a function of the collision centrality, of charged pions, kaons and (anti)protons from low (hundreds of MeV/c) [18] to high (20 GeV/c) [12] p_T . This is illustrated in Fig.2, where results for pp, the most central and the most peripheral Pb–Pb collisions are shown.

From the Blast-Wave analysis [19] applied to the low p_T part of the spectra, the radial flow, $\langle \beta_T \rangle$, in the most central collisions is found to be $\approx 10\%$ higher than

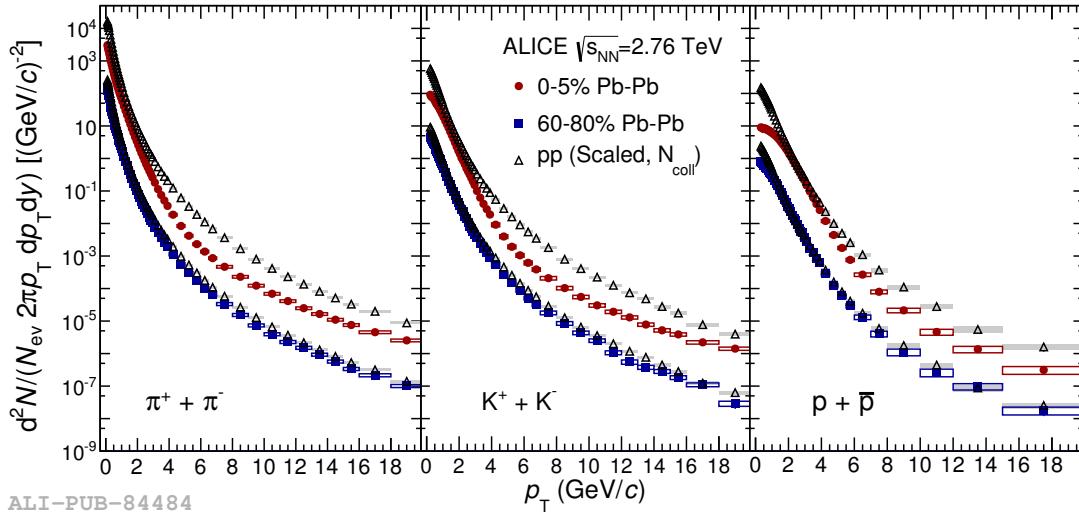


Figure 2: Solid markers show the invariant yields of identified particles in central (circles) and peripheral (squares) Pb–Pb collisions. Open points show the pp reference yields scaled by the average number of binary collisions for 0-5% (circles) and 60-80% (squares). The statistical and systematic uncertainties are shown as vertical error bars and boxes, respectively. Figure reproduced from Ref. [12].

at RHIC, while the kinetic freeze-out temperature was found to be comparable to that extracted from data at RHIC, $T_{\text{kin}} = 95$ MeV [18]. The spectra are well described by hydrodynamic models, except the low p_T (< 1 GeV/c) proton yield [20, 21, 22, 23]. Models which best describe the data include hadronic rescattering with non-negligible antibaryon annihilation [22, 23]. For intermediate to high p_T (> 3 GeV/c), the spectra develop the power law tail which characterizes the hard partonic processes.

The particle ratios as a function of p_T are shown in Fig. 3 for pp and the most central Pb–Pb collisions. The proton-to-pion ratio increases from ≈ 0.38 to ≈ 0.8 going from peripheral (60-80%) to central (0-5%) Pb–Pb collisions at $p_T \approx 3$ GeV/c, then decreases to the value measured for vacuum fragmentation (pp collisions) for $p_T > 10$ GeV/c. The result obtained for the most central collisions is similar to that measured at RHIC [24, 25]. The kaon-to-pion ratio also exhibits a bump around $p_T = 3$ GeV/c, this effect is not predicted by quark recombination suggesting that the actual enhancement of the baryon-to-meson ratio is not anomalous and instead it is most likely driven by hydrodynamical flow. This picture is tested by comparing the shapes of the p_T distributions of ϕ -meson and protons. The results shown in Fig. 4 indicate that for central Pb–Pb collisions the shapes of the ratios to pions are the same. Also shown is the evolution with collision centrality of the ϕ -meson yield normalized to that for protons as a function of p_T .

For p_T below 4 GeV/c the ratio become flat with the decreasing of the impact parameter. This suggests that the mass, and not the number of quark constituents, determines the spectral shape in central Pb–Pb collisions, this is in a good agreement with the hydro interpretation.

From the behavior of the particle ratios in both colliding systems one can establish that the suppression of the three particle species at high p_T (> 10 GeV/c) is the same within the statistical and systematic uncertainties. This suggests that the chemical composition of leading particles from jets in the medium is similar to that of vacuum jets. Another result concerning jet-quenching is the first indication for the mass dependence of the parton energy-loss, this by comparing the nuclear modification factor of the prompt D mesons to that for non-prompt J/ψ measured by CMS.

The elliptic flow for identified hadrons has been also measured [26] over a broad p_T range. Figure 5 shows v_2^1 as a function of p_T for central (10-20%) and semi-peripheral (40-50%) Pb–Pb collisions. Going from central to semi-peripheral Pb–Pb collisions v_2 increases as expected due to the eccentricity increase. For p_T below 2 GeV/c a mass ordering is observed indicating the interplay between elliptic and radial flow. For

¹The elliptic flow coefficients were obtained with the Scalar Product method, a two-particle correlation technique, using a pseudo-rapidity gap of $|\Delta\eta| > 0.9$ between the identified hadron under study and the reference particles [26].

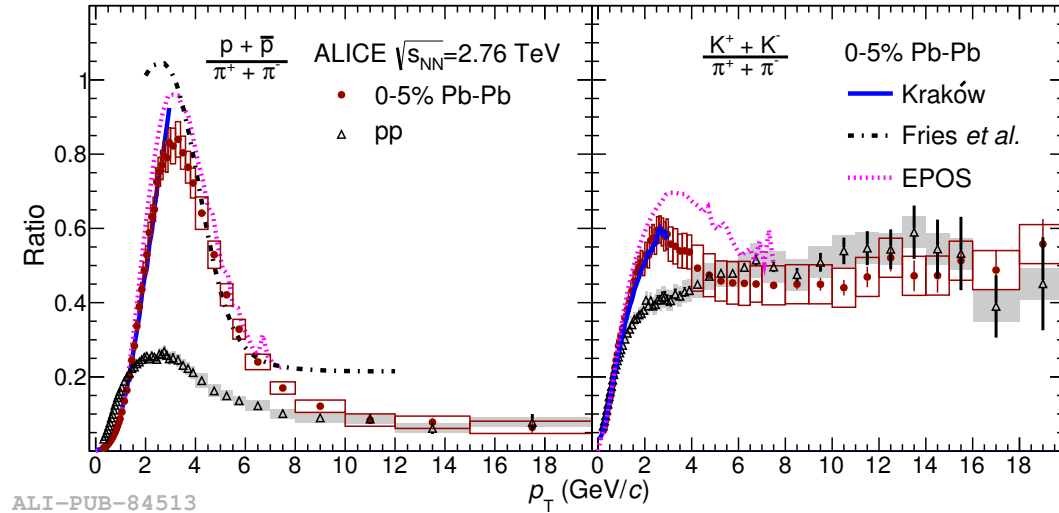


Figure 3: Particle ratios as a function of p_T measured in pp and the most central, 0-5%, Pb-Pb collisions. Statistical and systematic uncertainties are displayed as vertical error bars and boxes, respectively. The theoretical predictions refer to Pb-Pb collisions. Figure reproduced from Ref. [12].

higher p_T hadron- v_2 's seem to be grouped into baryons and mesons, the exception is the v_2 of ϕ -mesons, which for central Pb-Pb collisions follows that for baryons. This observation indicates that the behavior of v_2 is driven by the hadron mass and not for the number of quark constituents. ALICE has also reported the violation of the scaling of v_2 with the number of constituent quarks, such a observation is also against the scenario with quark recombination/coalescence.

4. Features of the “cold” matter

Surprisingly, early results from LHC showed that p-Pb collisions exhibit behaviors reminiscent to those due to final state effects, namely, hints of collective effects (radial and elliptic flow, ridge structure), but no sign of jet quenching [27, 28].

For p-Pb collisions the transverse momentum spectra of charged pions, kaons and (anti)protons as a function of the multiplicity measured in the VZERO-A detector have been reported from hundreds of MeV/c [28] up to 15 GeV/c [29]. At high multiplicity the low p_T parts of the spectra are better described by models which incorporate hydro [28]. Also intriguing is the fact that a similar effect has been observed in pp collisions, in that case the multiplicity was determined at mid-rapidity. The feature is also present in Pythia 8 tune 4C [30], this behavior is a consequence of the interactions among final partons coming from independent semi-hard scatterings which increases with increasing number of multi-parton

interactions (MPI) [31]. One therefore cannot rule out alternative explanations, but interestingly, it illustrates that likely there is a strong coupling of this phenomenon to the underlying event also in pp collisions.

The evolution of the spectral shapes with multiplicity is studied using the blast-wave analysis. Figure 6 (left) shows that a qualitatively similar behavior for T_{kin} vs. $\langle\beta_T\rangle$ is obtained for the three systems (pp, p-Pb and Pb-Pb) even in pp events simulated with Pythia 8. To study the effect on the p_T spectra directly, the proton-to-pion ratio was constructed, the results for p-Pb and Pb-Pb collisions are presented in Fig. 6 (right) for two extreme multiplicity intervals. For p_T below (above) 2 GeV/c the ratios exhibit a depletion (enhancement) going from low to high multiplicity. The highest (lowest) multiplicity intervals give ratios which reach maxima at $p_T \approx 3$ GeV/c amounting to ≈ 0.4 and ≈ 0.8 (≈ 0.28 and ≈ 0.38) in p-Pb and Pb-Pb collisions, respectively. Above 3 GeV/c, the ratios start to decrease down to ≈ 0.1 at $p_T \approx 10$ GeV/c, which according to [12] corresponds to the value measured for vacuum fragmentation (pp collisions).

Figure 7 shows the average p_T for K^{*0} , protons and ϕ -mesons as a function of the system size. The measurements were performed for pp, p-Pb and Pb-Pb collisions at $\sqrt{s_{NN}} = 7, 5.02$ and 2.76 TeV, respectively. The $\langle p_T \rangle$ for MB pp collisions fits well with the behavior of the p-Pb results. Actually, for inclusive charged particles a similar effect is seen, namely, the average p_T for pp and p-Pb data agree when the event multiplicity ($|\eta| < 0.3$) is

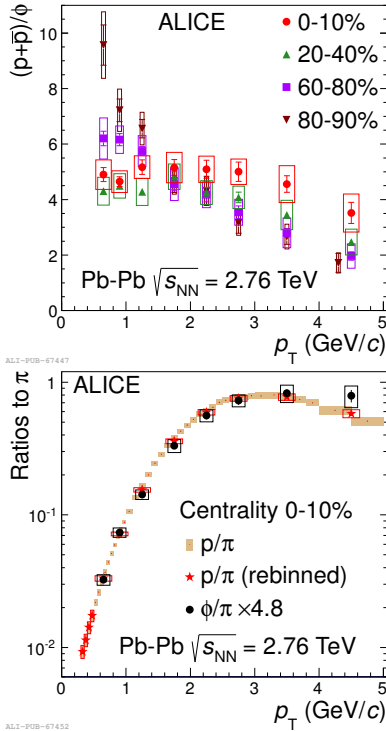


Figure 4: Ratio p/ϕ as a function of p_T for Pb–Pb collisions at 2.76 TeV for four centrality intervals. The statistical uncertainties are shown as bars and the total systematic uncertainties (including p_T -uncorrelated and p_T -correlated components) are shown as boxes (top). Ratios of proton and ϕ -meson yields to charged pion yield as a function of p_T for central Pb–Pb collisions at 2.76 TeV. In order to show the similarity of the shapes of the two ratios for $p_T < 3$ GeV/c, the ϕ/π ratio has been scaled so that the ϕ -meson and proton integrated yields are identical (bottom).

below ~ 20 , and for higher multiplicities the strongest rise of $\langle p_T \rangle$ is observed for pp data[32]. For Pb–Pb collisions the rise of $\langle p_T \rangle$ with the event multiplicity is weaker than for small systems. This could indicate that to reach the high multiplicity in small systems, the partonic processes need to be harder.

Another interesting result is shown in Fig. 8, where the multiplicity dependence of the proton-to- ϕ ratio as a function of p_T is shown. The p-Pb results are compared to the ratios measured in peripheral and central Pb–Pb collisions. The ratio for high multiplicity p-Pb events exhibits a flattening for p_T below 1.5 GeV/c, while for higher p_T the ratio decreases in the same amount as those measured for low multiplicity p-Pb and the most peripheral Pb–Pb collisions. The behavior of the ratio in high multiplicity p-Pb data could be interpreted as a hint of the onset of collective behavior.

Another feature of the p-Pb data is the non-zero el-

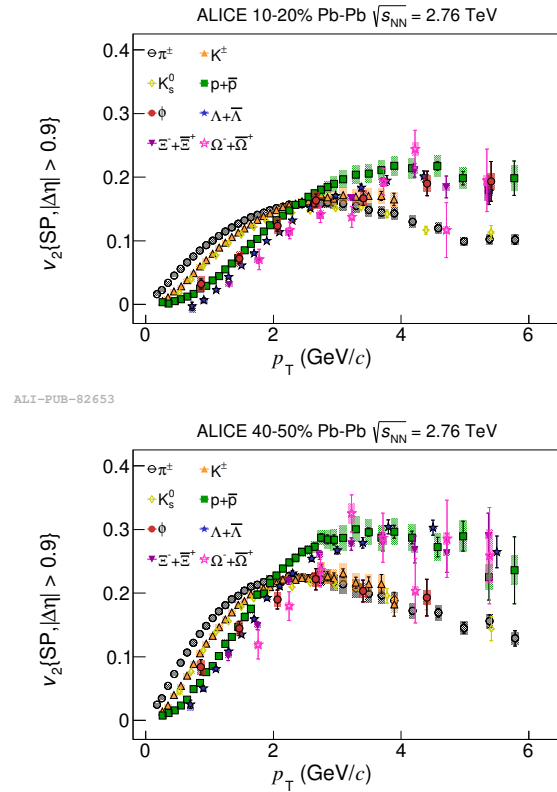


Figure 5: Elliptic flow coefficient (v_2) of identified hadrons as a function of p_T measured for central (top) and peripheral (bottom) Pb–Pb collisions.

liptic flow coefficient, right panel of Fig.8 shows that the p_T differential v_2 exhibits a mass ordering and a crossing for p_T around 1.5-2 GeV/c, again this feature is well known from heavy ion collisions. The results are reported in this paper [27]. To understand the potential role of MPI in p-Pb collisions the minijet production as a function of the event multiplicity was studied. In pp data this analysis was successfully applied. Through the measurement of the so-called number of uncorrelated seeds, which in Pythia are directly related with the number of MPIs, it was observed a deviation of this quantity with respect to the linear behavior, this was interpreted as an indication of the limitation of the number of MPIs to produce high multiplicity events [33]. Contrary, in p-Pb data a clear linear behavior at high multiplicity was observed, this could indicate the presence of MPIs in this colliding-systems [34].

To close this section it is important to mention the first measurements which were published at the LHC for high multiplicity pp data. The CMS Collaboration

reported the discovery of the ridge structure in high multiplicity events. At the same time, ALICE measured the average transverse sphericity, S_T [35], as a function of the event multiplicity [36], in this case it was shown that at high multiplicity $\langle S_T \rangle$ in data exhibit an opposite behavior to those predicted by QCD-inspired models. This can be interpreted in terms of an overestimation (by models) of the high p_T jet production. To understand the origin of these effects (flow patterns, ridge, sphericity) more detailed studies need to be done, this is one of the main topics with is being exploited in ALICE.

5. Summary

In Pb–Pb collisions, the presented results significantly improve the precision of previous measurements in various areas. In particular, a measurement of elliptic flow with identified particles shows a clear mass ordering for light and strange hadrons for $p_T < 2.5$ GeV/c. Spectra and v_2 measurements of the ϕ meson suggests that the mass (and not the number of constituent quarks) drives the spectral shape and the size of the elliptic flow in central collisions for $p_T < 4$ GeV/c. While there are several observables which are approximately consistent with a description of p–Pb collisions as incoherent superposition of nucleon–nucleon collisions at high p_T , some measurements hint to novel effects at low p_T which are potentially of collective origin. These findings still need to be reconciled theoretically and promise that p–Pb collisions will continue to be a very exciting field in the future.

References

- [1] P. Braun-Munzinger, J. Wambach, The Phase Diagram of Strongly-Interacting Matter, *Rev.Mod.Phys.* 81 (2009) 1031–1050. [arXiv:0801.4256](#), [doi:10.1103/RevModPhys.81.1031](#).
- [2] S. Borsanyi, et al., Is there still any T_c mystery in lattice QCD? Results with physical masses in the continuum limit III, *JHEP* 1009 (2010) 073. [arXiv:1005.3508](#), [doi:10.1007/JHEP09\(2010\)073](#).
- [3] C. Bernard, T. Burch, C. DeTar, J. Osborn, S. Gottlieb, E. Gregory, D. Toussaint, U. Heller, R. Sugar, Qcd thermodynamics with three flavors of improved staggered quarks, *Phys. Rev. D* 71 (2005) 034504. [doi:10.1103/PhysRevD.71.034504](#). URL <http://link.aps.org/doi/10.1103/PhysRevD.71.034504>
- [4] M. Cheng, N. Christ, S. Datta, J. van der Heide, C. Jung, F. Karsch, O. Kaczmarek, E. Laermann, R. Mawhinney, C. Miao, P. Petreczky, K. Petrov, C. Schmidt, T. Umeda, Transition temperature in qcd, *Phys. Rev. D* 74 (2006) 054507. [doi:10.1103/PhysRevD.74.054507](#). URL <http://link.aps.org/doi/10.1103/PhysRevD.74.054507>
- [5] T. Bhattacharya, M. I. Buchoff, N. H. Christ, H.-T. Ding, R. Gupta, C. Jung, F. Karsch, Z. Lin, R. D. Mawhinney, G. McGlynn, S. Mukherjee, D. Murphy, P. Petreczky, D. Renfrew, C. Schroeder, R. A. Soltz, P. M. Vranas, H. Yin, Qcd phase transition with chiral quarks and physical quark masses, *Phys. Rev. Lett.* 113 (2014) 082001. [doi:10.1103/PhysRevLett.113.082001](#). URL <http://link.aps.org/doi/10.1103/PhysRevLett.113.082001>
- [6] A. Bazavov, T. Bhattacharya, M. Cheng, C. DeTar, H.-T. Ding, S. Gottlieb, R. Gupta, P. Hegde, U. Heller, F. Karsch, E. Laermann, L. Levkova, S. Mukherjee, P. Petreczky, C. Schmidt, R. Soltz, W. Soeldner, R. Sugar, D. Toussaint, W. Unger, P. Vranas, Chiral and deconfinement aspects of the qcd transition, *Phys. Rev. D* 85 (2012) 054503. [doi:10.1103/PhysRevD.85.054503](#). URL <http://link.aps.org/doi/10.1103/PhysRevD.85.054503>
- [7] A. Ayala, A. Bashir, J. Cobos-Martinez, S. Hernandez-Ortiz, A. Raya, The effective QCD phase diagram and the critical end point [arXiv:1411.4953](#).
- [8] U. Heinz, C. Shen, H. Song, The viscosity of quark-gluon plasma at RHIC and the LHC, *AIP Conf.Proc.* 1441 (2012) 766–770. [arXiv:1108.5323](#), [doi:10.1063/1.3700674](#).
- [9] A. Collaboration, B. Alessandro, F. Antinori, J. A. Belikov, C. Blume, A. Dainese, P. Foka, P. Giubellino, B. Hippolyte, C. Kuhn, G. Martínez, M. Monteno, A. Morsch, T. K. Nayak, J. Nystrand, M. L. Noriega, G. Paic, J. Pluta, L. Ramello, J.-P. Revol, K. Safarik, J. Schukraft, Y. Schutz, E. Scapparini, R. Snellings, O. V. Baillie, E. Vercellin, Alice: Physics performance report, volume ii, *Journal of Physics G: Nuclear and Particle Physics* 32 (10) (2006) 1295. URL <http://stacks.iop.org/0954-3899/32/i=10/a=001>
- [10] M. Wilde, Measurement of Direct Photons in pp and Pb–Pb Collisions with ALICE, *Nucl. Phys. A* 904–905 (2013) 573c–576c. [arXiv:1210.5958](#), [doi:10.1016/j.nuclphysa.2013.02.079](#).
- [11] K. Aamodt, et al., Centrality dependence of the charged-particle multiplicity density at mid-rapidity in Pb–Pb collisions at $\sqrt{s_{NN}} = 2.76$ TeV, *Phys.Rev.Lett.* 106 (2011) 032301. [arXiv:1012.1657](#), [doi:10.1103/PhysRevLett.106.032301](#).
- [12] Production of charged pions, kaons and protons at large transverse momenta in pp and pb–pb collisions at 2.76 tev, *Physics Letters B* 736 (0) (2014) 196 – 207. [doi:http://dx.doi.org/10.1016/j.physletb.2014.07.011](#). URL <http://www.sciencedirect.com/science/article/pii/S0370269314004973>
- [13] B. B. Abelev, et al., Two-pion bose-einstein correlations in central pbpb collisions at, *Physics Letters B* 696 (4) (2011) 328 – 337. [doi:http://dx.doi.org/10.1016/j.physletb.2010.12.053](#). URL <http://www.sciencedirect.com/science/article/pii/S0370269310014565>
- [14] M. Floris, Hadron yields and the phase diagram of strongly interacting matter [arXiv:1408.6403](#), [doi:10.1016/j.nuclphysa.2014.09.002](#).
- [15] R. J. Fries, V. Greco, P. Sorensen, Coalescence Models For Hadron Formation From Quark Gluon Plasma, *Ann. Rev. Nucl. Part. Sci.* 58 (2008) 177–205. [arXiv:0807.4939](#), [doi:10.1146/annurev.nucl.58.110707.171134](#).
- [16] S. Sapeta, U. A. Wiedemann, Jet hadrochemistry as a characteristics of jet quenching, *Eur. Phys. J. C* 55 (2008) 293–302. [arXiv:0707.3494](#), [doi:10.1140/epjc/s10052-008-0592-8](#).

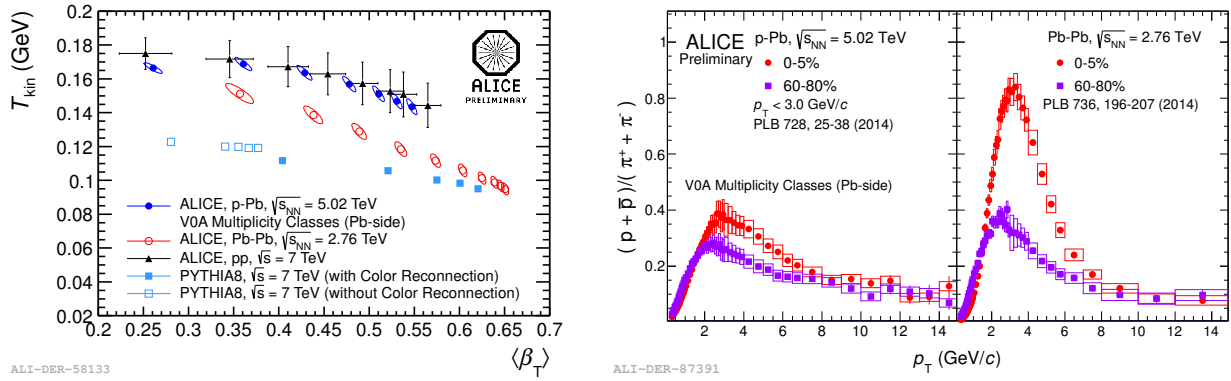


Figure 6: Comparison of the results from the blast-wave analysis applied to all available systems: pp, p-Pb and Pb–Pb collisions. The spectral shape analysis was also applied to Pythia 8 events. Charged-particle multiplicity increases from left to right. (Right.) Proton-to-pion ratio as a function of p_T measured in p-Pb and Pb–Pb collisions at $\sqrt{s_{NN}} = 5.02$ and 2.76 TeV, respectively. The systematic and statistical uncertainties are plotted as boxes and error bars, respectively.

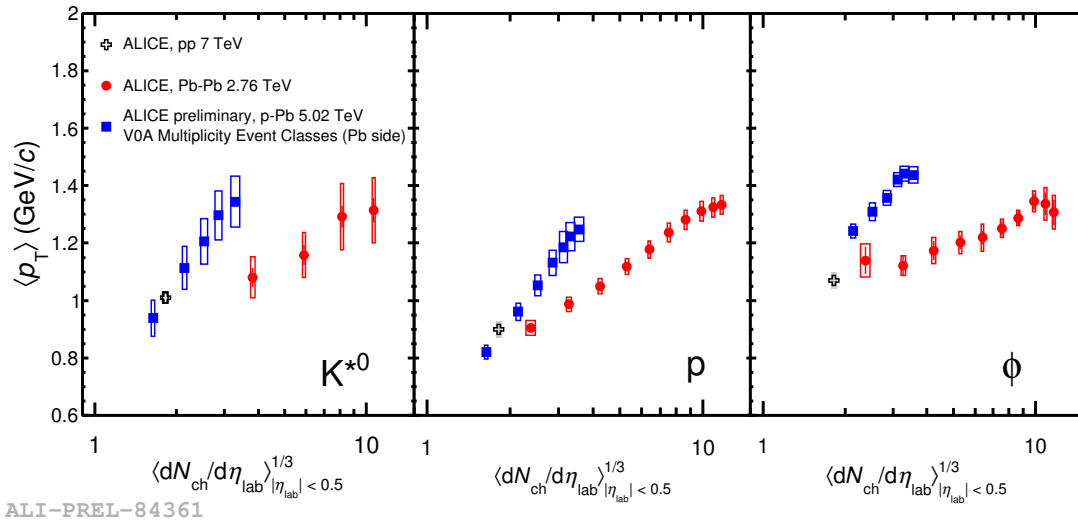


Figure 7: Mean transverse momentum of resonances compared to that of proton in the three different collision systems, as a function of the system size.

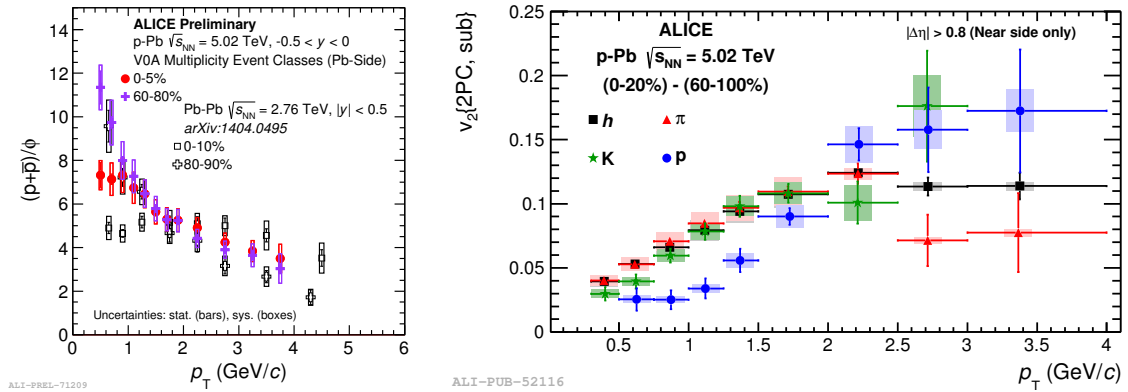


Figure 8: (Left). Ratios of proton yields to ϕ -meson yields vs p_T in p-Pb collision at 5.02 TeV and comparison with Pb–Pb. (Right). The Fourier coefficient v_2 for hadrons (black squares), pions (red triangles), kaons (green stars) and protons (blue circles) as a function of p_T from the correlation in the 0-20% multiplicity class after subtraction of the correlation from the 60-100% multiplicity class. Error bars show statistical uncertainties while shaded areas denote systematic uncertainties.

- [17] R. Bellwied, C. Markert, In-medium hadronization in the deconfined matter at RHIC and LHC, *Phys. Lett. B* 691 (2010) 208–213. [arXiv:1005.5416](#), [doi:10.1016/j.physletb.2010.06.028](#).
- [18] B. Abelev, et al., Centrality dependence of π , K, p production in Pb-Pb collisions at $\sqrt{s_{NN}} = 2.76$ TeV, *Phys. Rev. C* 88 (2013) 044910. [arXiv:1303.0737](#), [doi:10.1103/PhysRevC.88.044910](#).
- [19] E. Schnedermann, J. Sollfrank, U. Heinz, Thermal phenomenology of hadrons from 200a gev s+s collisions, *Phys. Rev. C* 48 (1993) 2462–2475. [doi:10.1103/PhysRevC.48.2462](#). URL <http://link.aps.org/doi/10.1103/PhysRevC.48.2462>
- [20] P. Bozek, I. Wyskiel-Piekarska, Particle spectra in Pb-Pb collisions at $\sqrt{s_{NN}} = 2.76$ TeV, *Phys. Rev. C* 85 (2012) 064915. [arXiv:1203.6513](#), [doi:10.1103/PhysRevC.85.064915](#).
- [21] I. Karpenko, Y. Sinyukov, K. Werner, Uniform description of bulk observables in hydrokinetic model of A + A collisions at RHIC and LHC, *Phys. Rev. C* 87 (2013) 024914. [arXiv:1204.5351](#), [doi:10.1103/PhysRevC.87.024914](#).
- [22] K. Werner, I. Karpenko, M. Bleicher, T. Pierog, S. Porteboeuf-Houssais, Jets, Bulk Matter, and their Interaction in Heavy Ion Collisions at Several TeV, *Phys. Rev. C* 85 (2012) 064907. [arXiv:1203.5704](#), [doi:10.1103/PhysRevC.85.064907](#).
- [23] C. Shen, U. Heinz, P. Huovinen, H. Song, Radial and elliptic flow in Pb+Pb collisions at the Large Hadron Collider from viscous hydrodynamic, *Phys. Rev. C* 84 (2011) 044903. [arXiv:1105.3226](#), [doi:10.1103/PhysRevC.84.044903](#).
- [24] A. Adare, et al., Spectra and ratios of identified particles in Au+Au and d+Au collisions at $\sqrt{s_{NN}}=200$ GeV, *Phys. Rev. C* 88 (2013) 024906. [arXiv:1304.3410](#), [doi:10.1103/PhysRevC.88.024906](#).
- [25] B. Abelev, et al., Identified baryon and meson distributions at large transverse momenta from Au+Au collisions at $\sqrt{s_{NN}} = 200$ -GeV, *Phys. Rev. Lett.* 97 (2006) 152301. [arXiv:nucl-ex/0606003](#), [doi:10.1103/PhysRevLett.97.152301](#).
- [26] B. B. Abelev, et al., Elliptic flow of identified hadrons in Pb-Pb collisions at $\sqrt{s_{NN}} = 2.76$ TeV [arXiv:1405.4632](#).
- [27] B. B. Abelev, et al., Long-range angular correlations of π , K and p in p–Pb collisions at $\sqrt{s_{NN}} = 5.02$ TeV, *Phys. Lett. B* 726 (2013) 164–177. [arXiv:1307.3237](#), [doi:10.1016/j.physletb.2013.08.024](#).
- [28] B. B. Abelev, et al., Multiplicity Dependence of Pion, Kaon, Proton and Lambda Production in p-Pb Collisions at $\sqrt{s_{NN}} = 5.02$ TeV, *Phys. Lett. B* 728 (2014) 25–38. [arXiv:1307.6796](#), [doi:10.1016/j.physletb.2013.11.020](#).
- [29] A. Ortiz Velasquez, Production of $\pi/K/p$ from intermediate to high p_T in pp, p-Pb and Pb-Pb collisions measured by ALICE [arXiv:1404.4354](#).
- [30] R. Corke, T. Sjostrand, Interleaved Parton Showers and Tuning Prospects, *JHEP* 1103 (2011) 032. [arXiv:1011.1759](#), [doi:10.1007/JHEP03\(2011\)032](#).
- [31] A. Ortiz Velasquez, P. Christiansen, E. Cuautle Flores, I. Maldonado Cervantes, G. Paic, Color Reconnection and Flow-like Patterns in pp Collisions, *Phys. Rev. Lett.* 111 (4) (2013) 042001. [arXiv:1303.6326](#), [doi:10.1103/PhysRevLett.111.042001](#).
- [32] B. B. Abelev, et al., Multiplicity dependence of the average transverse momentum in pp, p-Pb, and Pb-Pb collisions at the LHC, *Phys. Lett. B* 727 (2013) 371–380. [arXiv:1307.1094](#), [doi:10.1016/j.physletb.2013.10.054](#).
- [33] B. Abelev, et al., Multiplicity dependence of two-particle azimuthal correlations in pp collisions at the LHC, *JHEP* 1309 (2013) 049. [arXiv:1307.1249](#), [doi:10.1007/JHEP09\(2013\)049](#).
- [34] B. B. Abelev, et al., Multiplicity dependence of jet-like two-particle correlations in p-Pb collisions at $\sqrt{s_{NN}} = 5.02$ TeV [arXiv:1406.5463](#).
- [35] E. Cuautle, R. Jimenez, I. Maldonado, A. Ortiz, G. Paic, et al., Disentangling the soft and hard components of the pp collisions using the sphero(i)city approach [arXiv:1404.2372](#).
- [36] B. Abelev, et al., Transverse sphericity of primary charged particles in minimum bias proton-proton collisions at $\sqrt{s} = 0.9, 2.76$ and 7 TeV, *Eur. Phys. J. C* 72 (2012) 2124. [arXiv:1205.3963](#), [doi:10.1140/epjc/s10052-012-2124-9](#).